Fabrication and characterization of chalcogenide glass photonic crystal waveguides

Keijiro Suzuki,[1,2] Yohei Hamachi,[1,2] and Toshihiko Baba[1,2,*]

[1]*Department of Electrical and Computer Engineering, Yokohama National University,
79-5 Tokiwadai, Hodogaya-ku, Yokohama, 240-8501, Japan*
[2]*Core Research for Evolutional Science and Technology, Japan Science and Technology Agency,
5 Sanbancho, Chiyoda-ku, Tokyo, 102-0075, Japan*
*baba@ynu.ac.jp

Abstract: We report on the fabrication of chalcogenide glass (Ag-As$_2$Se$_3$) photonic crystal waveguides and the first detailed characterization of the linear and nonlinear optical properties. The waveguides, fabricated by *e*-beam lithography and ICP etching exhibit typical transmission spectra of photonic crystal waveguides, and exhibit high optical nonlinearity. Nonlinear phase shift of 1.5π through self-phase modulation is observed at 0.78 W input peak power in a 400 μm long device. The effective nonlinear parameter γ_{eff} estimated from this result reaches 2.6×10^4 W^{-1}m^{-1}. Four-wave mixing is also observed in the waveguide, while two-photon absorption at optical communication wavelengths is sufficiently small and the corresponding figure of merit is larger than 11.

OCIS codes: (230.5298) Photonic crystals; (160.2750) Glass and other amorphous materials; (230.3120) Integrated optics devices; (230.4320) Nonlinear optical devices.

References and links

1. J. M. Harbold, F. O. Ilday, F. W. Wise, J. S. Sanghera, V. Q. Nguyen, L. B. Shaw, and I. D. Aggarwal, "Highly nonlinear As-S-Se glasses for all-optical switching," Opt. Lett. **27**(2), 119–121 (2002).
2. A. Zakery, and S. R. Elliott, "Optical properties and applications of chalcogenide glasses: a review," J. Non-Cryst. Solids **330**(1-3), 1–12 (2003).
3. A. V. Rode, A. Zakery, M. Samoc, R. B. Charters, E. G. Gamaly, and B. Luther-Davies, "Laser-deposited As$_2$S$_3$ chalcogenide films for waveguide applications," Appl. Surf. Sci. **197-198**, 481–485 (2002).
4. T. G. Robinson, R. G. DeCorby, J. N. McMullin, C. J. Haugen, S. O. Kasap, and D. Tonchev, "Strong Bragg gratings photoinduced by 633-nm illumination in evaporated As$_2$Se$_3$ thin films," Opt. Lett. **28**(6), 459–461 (2003).
5. D. Freeman, C. Grillet, M. W. Lee, C. L. C. Smith, Y. Ruan, A. Rode, M. Krolikowska, S. Tomljenovic-Hanic, C. M. De Sterke, M. J. Steel, B. Luther-Davies, S. Madden, D. J. Moss, Y. H. Lee, and B. J. Eggleton, "Chalcogenide glass photonic crystals," Photon. Nanostructures **6**, 3–11 (2008).
6. V. G. Ta'eed, N. J. Baker, L. B. Fu, K. Finsterbusch, M. R. E. Lamont, D. J. Moss, H. C. Nguyen, B. J. Eggleton, D. Y. Choi, S. Madden, and B. Luther-Davies, "Ultrafast all-optical chalcogenide glass photonic circuits," Opt. Express **15**(15), 9205–9221 (2007), http://www.opticsinfobase.org/oe/abstract.cfm?URI=oe-15-15-9205.
7. K. Ogusu, J. Yamasaki, S. Maeda, M. Kitao, and M. Minakata, "Linear and nonlinear optical properties of Ag-As-Se chalcogenide glasses for all-optical switching," Opt. Lett. **29**(3), 265–267 (2004).
8. K. Suzuki, K. Ogusu, and M. Minakata, "Single-mode Ag-As$_2$Se$_3$ strip-loaded waveguides for applications to all-optical devices," Opt. Express **13**(21), 8634–8641 (2005), http://www.opticsinfobase.org/oe/abstract.cfm?URI=oe-13-21-8634.
9. T. Baba, "Slow light in photonic crystals," Nat. Photonics **2**(8), 465–473 (2008).
10. Y. Hamachi, S. Kubo, and T. Baba, "Slow light with low dispersion and nonlinear enhancement in a lattice-shifted photonic crystal waveguide," Opt. Lett. **34**(7), 1072–1074 (2009).
11. B. Corcoran, C. Monat, C. Grillet, D. J. Moss, B. J. Eggleton, T. P. White, L. O'Faolain, and T. F. Krauss, "Green light emission in silicon through slow-light enhanced third-harmonic generation in photonic-crystal waveguides," Nat. Photonics **3**(4), 206–210 (2009).
12. C. Monat, B. Corcoran, M. Ebnali-Heidari, C. Grillet, B. J. Eggleton, T. P. White, L. O'Faolain, and T. F. Krauss, "Slow light enhancement of nonlinear effects in silicon engineered photonic crystal waveguides," Opt. Express **17**(4), 2944–2953 (2009), http://www.opticsinfobase.org/oe/abstract.cfm?URI=oe-17-4-2944.
13. A. Baron, A. Ryasnyanskiy, N. Dubreuil, P. Delaye, Q. Vy Tran, S. Combrié, A. de Rossi, R. Frey, and G. Roosen, "Light localization induced enhancement of third order nonlinearities in a GaAs photonic crystal waveguide," Opt. Express **17**(2), 552–557 (2009), http://www.opticsinfobase.org/oe/abstract.cfm?URI=oe-17-2-552.

14. K. Inoue, H. Oda, N. Ikeda, and K. Asakawa, "Enhanced third-order nonlinear effects in slow-light photonic-crystal slab waveguides of line-defect," Opt. Express **17**(9), 7206–7216 (2009), http://www.opticsinfobase.org/oe/abstract.cfm?URI=oe-17-9-7206.
15. D. Pudo, B. Corcoran, C. Monat, M. Pelusi, D. J. Moss, B. J. Eggleton, T. P. White, L. O'Faolain, and T. F. Krauss, "Investigation of slow light enhanced nonlinear transmission for all-optical regeneration in silicon photonic crystal waveguides at 10 Gbit/s," Photonic. Nanostruct," Corrected Proof. In Press., doi:10.1016/j.photonics.2009.08.002.
16. M. W. Lee, C. Grillet, C. G. Poulton, C. Monat, C. L. Smith, E. Mägi, D. Freeman, S. Madden, B. Luther-Davies, and B. J. Eggleton, "Characterizing photonic crystal waveguides with an expanded k-space evanescent coupling technique," Opt. Express **16**(18), 13800–13808 (2008), http://www.opticsinfobase.org/oe/abstract.cfm?URI=oe-16-18-13800.
17. T. Wagner, V. Perina, A. Mackova, E. Rauhala, A. Seppala, M. Vleck, S. O. Kasap, M. Vlcek, and M. Frumar, "The tailoring of the composition of Ag-As-S amorphous films using photo-induced solid state reaction between Ag and $As_{30}S_{70}$ films," Solid State Ion. **141-142**(1), 387–395 (2001).
18. G. P. Agrawal, *Nonlinear Fiber Optics,* Fourth ed. (Academic Press, London, 2007).
19. E. Dulkeith, Y. A. Vlasov, X. Chen, N. C. Panoiu, and R. M. Osgood, Jr., "Self-phase-modulation in submicron silicon-on-insulator photonic wires," Opt. Express **14**(12), 5524–5534 (2006), http://www.opticsinfobase.org/oe/abstract.cfm?URI=oe-14-12-5524.
20. J. M. Harbold, F. Ö. Ilday, F. W. Wise, J. S. Sanghera, V. Q. Nguyen, L. B. Shaw, and I. D. Aggarwal, "Highly nonlinear As-S-Se glasses for all-optical switching," Opt. Lett. **27**(2), 119–121 (2002).
21. R. W. Boyd, *Nonlinear Optics,* Third ed. (Academic Press, New York, 2008).
22. M. R. Lamont, B. Luther-Davies, D.-Y. Choi, S. Madden, X. Gai, and B. J. Eggleton, "Net-gain from a parametric amplifier on a chalcogenide optical chip," Opt. Express **16**(25), 20374–20381 (2008), http://www.opticsinfobase.org/oe/abstract.cfm?URI=oe-16-25-20374.
23. G. Lenz, J. Zimmermann, T. Katsufuji, M. E. Lines, H. Y. Hwang, S. Spälter, R. E. Slusher, S. W. Cheong, J. S. Sanghera, and I. D. Aggarwal, "Large Kerr effect in bulk Se-based chalcogenide glasses," Opt. Lett. **25**(4), 254–256 (2000).
24. H. Fukuda, K. Yamada, T. Shoji, M. Takahashi, T. Tsuchizawa, T. Watanabe, J. Takahashi, and S. Itabashi, "Four-wave mixing in silicon wire waveguides," Opt. Express **13**(12), 4629–4637 (2005), http://www.opticsinfobase.org/oe/abstract.cfm?URI=oe-13-12-4629.

1. Introduction

Chalcogenide glasses (ChGs) are based on chalcogen elements (S, Se and Te), mixed with other elements such as As, Ge, P and Sb. They are transparent at optical communication wavelengths, and exhibit high optical Kerr nonlinearity as well as low two-photon absorption (TPA) [1,2]. The nonlinearity is non-resonant, and has a subpicosecond response time. ChGs also exhibit several photoinduced phenomena when illuminated with light near the band-gap. By the use of these phenomena, the formation of waveguides and gratings [3,4] and post-tuning of photonic crystal waveguides [5] have been reported. In addition, integration with Si-photonics is also possible because ChGs can be formed and processed at low temperature (<400 °C). These characteristics make ChGs a promising platform for integrated all-optical devices [6]. Recently, it is found that Ag-doped As_2Se_3 glass (i.e., $Ag_x(As_{0.4}Se_{0.6})_{100-x}$) has particularly high Kerr nonlinearity higher than As_2Se_3 by around 2–4 times at wavelength $\lambda = 1053$ nm without increasing TPA coefficient [7], and low material absorption loss at infrared region [8]. We apply this glass in a guiding layer of our devices described below.

Photonic crystal waveguides (PCWs) consisting of photonic crystal slab and a line defect, are a useful platform for on-chip photonic devices and circuits. PCWs can enhance nonlinear effects by exploiting its small modal cross-section and slow light effect [9]. In SOI-based PCWs, self-phase modulation (SPM), two-photon absorption (TPA) and third harmonic generation have been observed [10–12]. In GaAs and AlGaAs-based PCWs, the enhancement of SPM and TPA is demonstrated [13,14]. PCWs have been finding applications for integrated nonlinear devices [15].

Further nonlinear enhancement is expected for the combination of the ChGs and PCWs. However, the difficulty in the fabrication has limited its experimental demonstration [5]. ChGs are much softer than Si, which makes difficult to obtain vertical sidewalls of air-holes and clean facets for efficient optical coupling to the waveguides. Hence, only their fundamental characteristics have been investigated under the limited condition [16], and their nonlinear characteristics have not been investigated yet.

In this study, we develop the fabrication technique of fine Ag-As_2Se_3 ChG PCW using *e*-beam lithography and ICP etching, and characterize their detailed linear and nonlinear optical

properties, for the first time. We successfully observed the light propagation characteristics of the waveguides. In addition, we confirmed the generation of SPM and the four-wave mixing (FWM) in the ChG PCW. Negligible TPA is also observed at optical communication wavelengths.

2. Design and fabrication

Figure 1(a) shows the schematic of ChG PCW, which consists of air-holes embedded in a Ag-As_2Se_3 layer. An InP substrate is used for easy cleavage. A Ti layer is used for better adhesion between As_2Se_3 and InP. Typical device length is 400 μm. To analyze waveguide modes, we used 3D-FDTD method. In this analysis, we assumed that refractive index of the slab is 2.85, the normalized air-hole diameter $2r/a$ is 0.52 and normalized slab thickness d/a is 0.63, where a is the lattice constant. Figures 1(b) and 1(c) show the three-dimensional photonic band diagram, which show the presence of guiding modes within the bandgap. Provided the light propagation at $\lambda = 1550$ nm, we obtain $a = 480$ nm, $2r = 250$ nm and $d = 300$ nm. These structural parameters indicate that the fabrication of ChG PCW is practical. The transmission bandwidth of even guided mode sandwiched by the air light cone and the band-edge completely covers the C band of silica fiber communications.
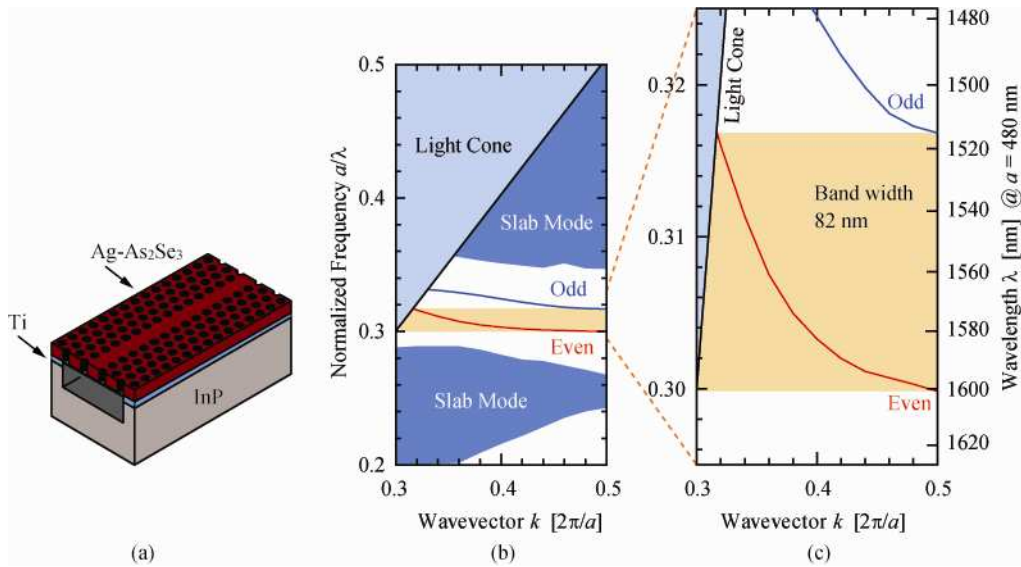

Fig. 1. (a) Schematic of chalcogenide glass photonic crystal waveguide. (b) Band diagram of Ag-As_2Se_3 photonic crystal waveguide. (c) Magnified figure of (b).

Figure 2 shows a fabrication process of ChG PCW. First, Ti layer is thermally evaporated onto an InP substrate by 10 nm at 6.0 nm/min. Then, commercially available As_2Se_3, Furuuchi Chemical is thermally evaporated onto the Ti layer by 300 nm at a rate of 10 nm/min. The Ag-As_2Se_3 layer cannot be obtained by direct evaporation of the ternary Ag-As-Se glass because of their phase difference. Therefore, Ag layer is evaporated on the As_2Se_3 layer by 10 nm, and doped into As_2Se_3 film using photodoping technique [17]. 10 nm thickness of Ag corresponds to an Ag content of 5 at.%. Next, standard e-beam lithography is used to pattern PCWs. An EB resist ZEP-520A, ZEON is spincasted onto the surface, and prebaked at 180 °C for 2 min. PCWs are patterned by e-beam accelerated by 50 kV. After development, the substrate is post-baked at 130 °C for 30 min. The pattern of PCW is transferred to Ag-As_2Se_3 layer by ICP etching (RIE-10iP, Samco). The etching gas is a CHF_3 and CF_4 mixture. After the etching, a residual EB resist on the surface of the guiding layer is removed by a cleaner solution. Finally, Ti and InP underneath the PCWs are removed by HF and successive HCl solution to form an air-bridge structure.

Figure 3 shows scanning electron microscope (SEM) image of the fabricated ChG PCW. The cross-sectional image shows that the air-holes have sufficiently smooth and vertical sidewalls, and the cleaved facet looks clean enough to couple external light to the waveguide efficiently. From the top view, it is evaluated that the fluctuation of air-hole diameter is ± 10 nm.
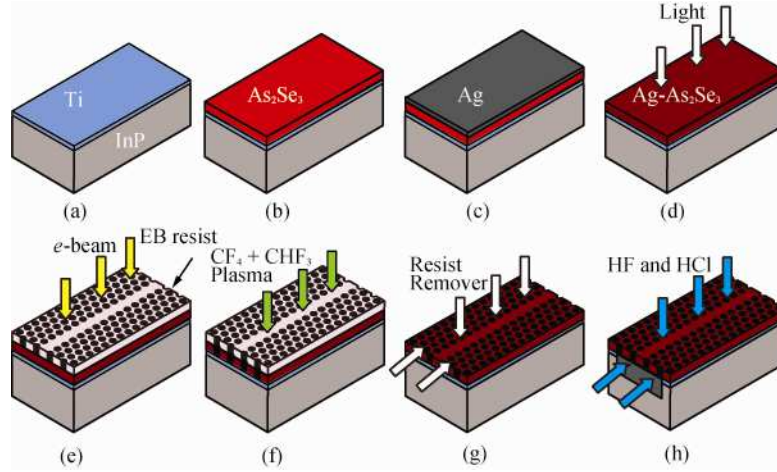

Fig. 2. Fabrication process of the Ag-As$_2$Se$_3$ chalcogenide glass photonic crystal waveguides. (a) Ti thermal evaporation. (b) As$_2$Se$_3$ thermal evaporation. (c) Ag thermal evaporation. (d) Photo-doping of Ag into As$_2$Se$_3$ using Halogen lamp. (e) EB writing of photonic crystal waveguides. (f) ICP etching using a CHF$_3$/CF$_4$ gas mixture. (g) EB resist removal using ZDMAC remover. (h) Wet-etching in HF and HCl solution.
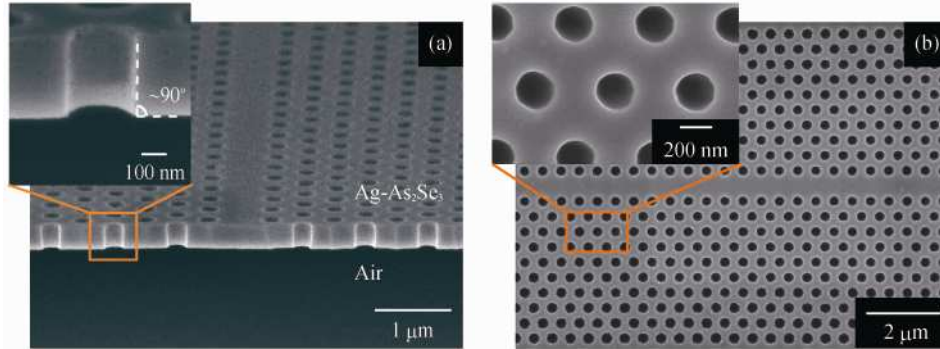

Fig. 3. SEM image of a fabricated Ag-As$_2$Se$_3$ photonic crystal waveguide. (a) Cross-sectional view. (b) Top view.

3. Measurement

3.1 Transmission spectrum

Figure 4 shows the transmission spectrum of a fabricated ChG PCW. Here, tunable laser light was coupled to the waveguide from the cleaved facet through microscope objectives. Transmission drops caused by the light line and band edge are confirmed, indicating that the obtained spectrum is a typical one of single line defect PCW. The transmission bandwidth defined by the light line and band edge is in good agreement with photonic band analysis shown in Fig. 1(c). The transmitted power is ~5 dB lower than the typical one of our 400-μm-long Si-PCW at λ = 1550 nm (corresponding to group index n_g ~5). In our Si-PCW, the propagation loss is typical 1 dB/mm, corresponding to 0.4 dB loss in a 400-μm-length

waveguide. In the ChG PCW, the loss of 400-μm-length waveguide is estimated to 5 + 0.4 = 5.4 dB. Hence, 5.4 dB/0.4 mm = 13.5 dB/mm is evaluated as the propagation loss of the ChG PCW.
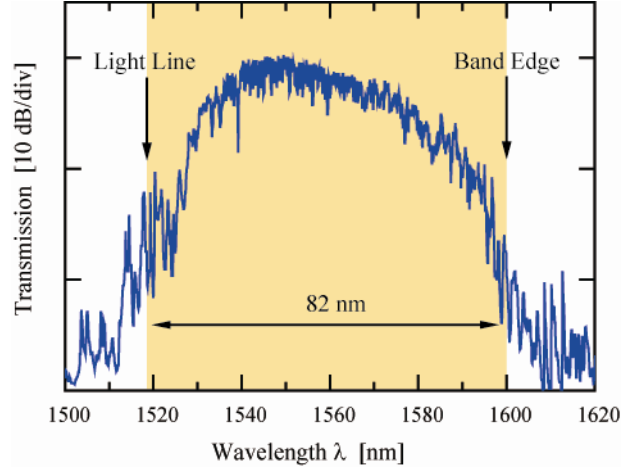

Fig. 4. Transmission spectrum of a fabricated chalcogenide glass photonic crystal waveguide.

3.2 Self-phase modulation

We observed SPM by launching optical pulses in the transmission band near the band-edge. In the SPM and TPA measurements, we used another sample which has a band-edge at λ ~1550 nm. Figure 5 shows experimental setup. The optical pulse from passive mode-locked laser was expanded spectrally by SPM at the first erbium-doped fiber amplifier (EDFA). Then, the pulse was filtered at desired center wavelength λ_p and pulse width τ_p. We chose λ_p = 1547 nm corresponding to the band edge of the sample (n_g = 10), and τ_p = 2.0 ps to suppress SPM in silica fibers of the setup. The filtered pulse was amplified by the second EDFA, and coupled to the PCW through the microscope objectives. The output pulse from the PCW was detected with a lensed fiber. The pulse spectrum was observed by an optical spectrum analyzer (OSA).

Figure 6 shows spectra of output pulse at different launched input peak powers P_{in} for 400-μm-long device. The SPM-induced spread spectrum is clearly observed when the coupled pulse peak power is higher than 0.63 W. The asymmetrical spreading of the spectra is caused by the cut-off at the band-edge. When we coupled pulses of P_{in} = 0.78 W to the PCW, the output pulse spectrum exhibited two peaks and center dip, indicating that the nonlinear phase change $\Delta\phi_{NL}$ = 1.5π [18]. This is the evidence of the large nonlinear enhancement of the ChG.

Let us compare the efficiency of the nonlinear phase change with Si-wire [19]. The Ag-As$_2$Se$_3$ PCW requires 0.78 W input peak power, 230 μm effective length L_{eff} (1/e power decay length for a propagation loss of 13.5 dB/mm, neglecting TPA) and 0.18 μm^2 cross-sectional area for 1.5π nonlinear phase shift. On the other hand, in Si-wire, the same phase shift is observed with 6.85 W peak power, 3400 μm effective length (propagation loss: 0.36 dB/mm) and 0.106 μm^2 cross-sectional area. That is, the Ag-As$_2$Se$_3$ PCW only needs nine times lower peak power, and 15 times shorter effective length and 1.7 times broader cross-sectional area. In total, it is 79 times more efficient than Si-wire.

To confirm the result, we also estimate the efficiency from material and structural parameters. Although the nonlinear refractive index n_2 of Ag-As$_2$Se$_3$ has not been measured at λ ~1550 nm, it has been reported in [7] that the Ag doping enhances n_2 to 2 − 4 times larger at λ = 1053 nm. Let us assume here that n_2 of Ag-As$_2$Se$_3$ is three times larger than 2300 × 10^{-20} m^2/W for As$_2$Se$_3$ [20], i.e. 6900 × 10^{-20} m^2/W, which is 26 times Si's (270 × 10^{-20} m^2/W) [21]. The nonlinear enhancement is proportional to n_g^2 [10,14]. Since n_g of the fabricated PCW and Si-wire are estimated to be 10 and 4.5, respectively, the enhancement is (10/4.5)^2 = 5 times.

Regarding the cross-sectional area, it is the same as mentioned above. In total, the fabricated PCW should be more efficient than Si-wire by $26 \times 5/1.7 = 76$ times. This value is in good agreement with the experimental value.
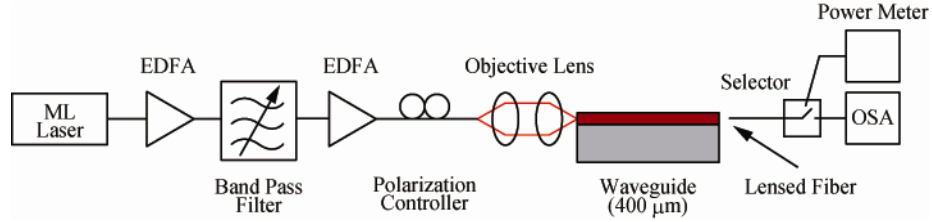

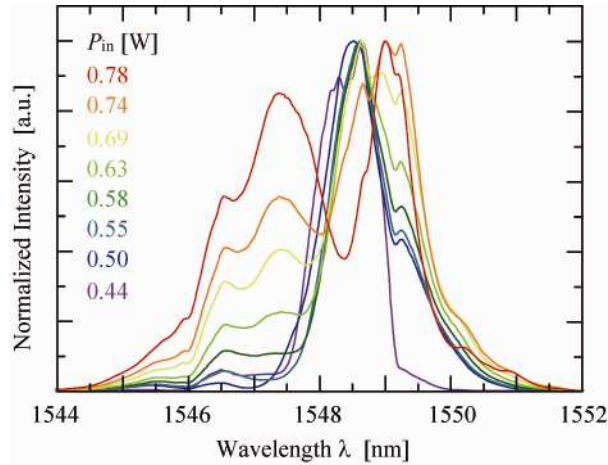
Fig. 5. Experimental setup for self-phase modulation.

Fig. 6. Spectra of output pulse exhibiting SPM. Each spectrum is normalized to the peak magnitude

In the same manner, we estimated the effective nonlinear parameter $\gamma_{eff} = \Delta\phi_{NL}/P_{in}L_{eff}$ to be 2.6×10^4 $W^{-1}m^{-1}$. This value is much larger than a reported value for As_2S_3 ChG rib-waveguide of 10 $W^{-1}m^{-1}$ [22]. The above n_2 for $Ag-As_2Se_3$ is already 23 times larger than 300×10^{-20} $W^{-1}m^{-1}$ for As_2S_3. Since n_g of the $Ag-As_2Se_3$ PCW and As_2S_3 rib-waveguide are estimated to 10 and 2.4, respectively, the enhancement is $(10/2.4)^2 = 17$ times. As for A_{eff}, we assumed that it is proportional to the cross-sectional area of the waveguide, i.e., 0.18 and 1.2 μm^2 for the PCW and rib-waveguide, respectively, corresponding to 7 times enhancement. In total, deduced γ_{eff} of the ChG PCW is $10 \times 23 \times 17 \times 7 = 2.7 \times 10^4$ $W^{-1}m^{-1}$. This also agrees well with the above value. Thus, all the comparisons are consistent with each other.

3.3 Two-photon absorption

We measured input/output characteristics of a ChG PCW to evaluate the TPA. The experiment setup was the same as for the SPM. Figure 7 shows the result. Note that the output power keeps linear when the input power is sufficiently high to generate the SPM, indicating that the TPA of $Ag-As_2Se_3$ is negligible in the optical communication wavelengths.

Nonlinear switching devices are designed to have a large figure of merit (FOM), which is defined as the nonlinearity per unit nonlinear absorption (i.e. FOM = $n_2/(\beta\lambda)$, where β is the TPA coefficient). The requirement for FOM depends on switching mechanisms, e.g. ~5 for Mach-Zehnder switches [23]. In bulk As_2Se_3, FOM is as high as ~11 [1]. Ag-doped As_2Se_3 exhibits not only high nonlinearity but negligible TPA. As the nonlinearity of $Ag-As_2Se_3$ is higher than As_2Se_3 by Ag doping, FOM > 11 is expected.
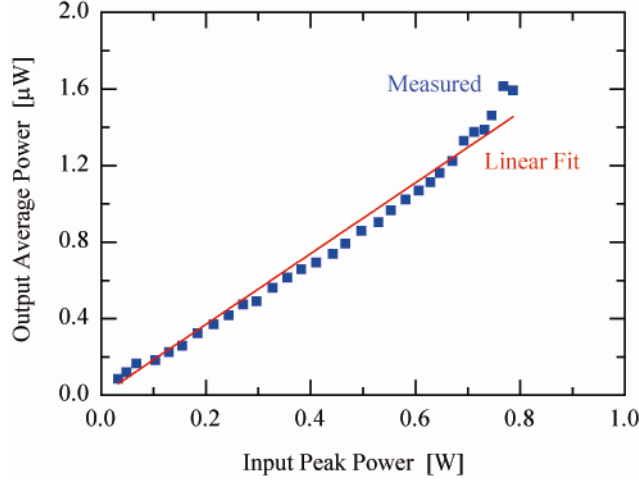
Fig. 7. Output average power versus input peak power characteristic.

3.4 Four-wave mixing

Figure 8 shows the experimental setup. We launched two optical pulses at different wavelengths as pump lights to generate FWM. The mode-locked laser pulse was expanded spectrally at the first EDFA, then divided by 3 dB coupler into two arms. The divided pulses were filtered at each band-pass filters as pump lights. The center wavelengths of the two pulses λ_1 (ω_1) and λ_2 (ω_2) were 1556 nm (192.7 THz) and 1560 nm (192.2 THz), respectively, both corresponding to the fast group velocity regime of the PCW. Their spectral width was suppressed to less than 2 nm to avoid the FWM in silica fibers of the setup. Then, they were amplified by following EDFA. A delay line was introduced into one arm to alter the timing of the confluence at a following 3 dB coupler. The timing of the two pulses was adjusted so that their auto-correlation trace exhibits the clearest beat. The pulses were coupled to the PCW through the microscope objectives. The output pulse was detected by a lensed fiber, and its spectrum was observed by the OSA.

Figure 9 shows spectra of the output pulse. Signal and idler light are observed around the two pumps when the input peak power increases. The center wavelengths of signal λ_{sig} (ω_{sig}) and idler λ_{idl} (ω_{idl}) light are 1552 (193.2 THz) nm and 1564 nm (191.7 THz), respectively, which is in good agreement with theoretically estimated values from frequency matching conditions ($\omega_{sig} = 2\omega_1 - \omega_2$, $\omega_{idl} = 2\omega_2 - \omega_1$). Considering the short device length (400 μm) and pulse propagation at the fast group velocity regime, this is another evidence of the large nonlinearity in the ChG.

In Si-wire [24], the FWM occurs with 0.2 W peak power (CW), 10200 μm effective length (propagation loss: 0.24 dB/mm) and 0.09 μm^2 cross-sectional area. In comparison with them, 1.7 times higher peak power, 1/44 times shorter effective length and a twice cross-sectional area give the similar FWM, corresponding to 13 times higher efficiency than Si-wire's.
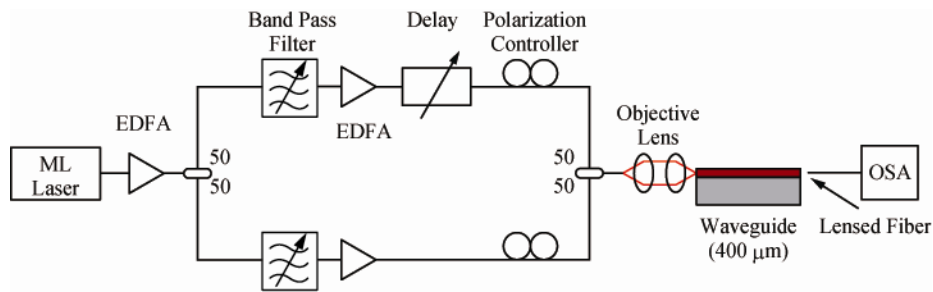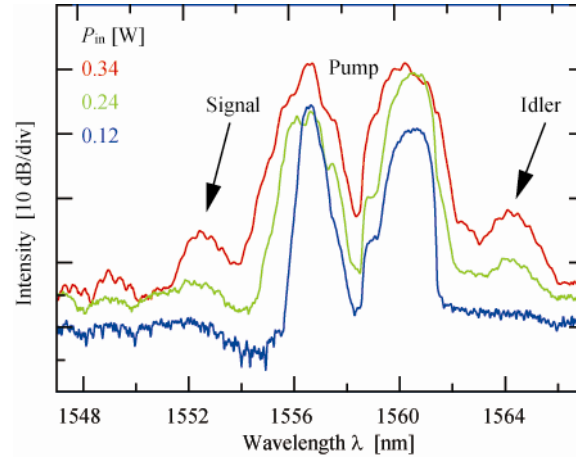
Fig. 8. Experimental setup for FWM.

Fig. 9. Spectra of output pulse exhibiting FWM in Ag-As$_2$Se$_3$ PCW.

4. Conclusion

We have fabricated Ag-As$_2$Se$_3$ chalcogenide glass photonic crystal waveguides and demonstrated large self-phase modulation, and four-wave mixing, and negligible two-photon absorption for the first time. The large effective nonlinear parameter (2.6×10^4 W^{-1}m^{-1}) is the clear evidence of the advantage of chalcogenide glass photonic crystal waveguides for all-optical switching devices. Further nonlinearity enhancement is expected by exploiting low dispersion slow-light structures.

Acknowledgements